ELSEVIER
Thermochimica Acta 262 (1995) 33–43
thermochimica
acta

Polymerization calorimeter. Part 2. Practical use and application in polymerizations

Mikko Lahti[a,*], Arno Avela[b], Jukka Seppälä[a]

[a] *Helsinki University of Technology, Department of Chemical Engineering, Laboratory of Industrial Chemistry and Polymer Technology, Kemistintie 1, FIN-02150 Espoo, Finland*
[b] *Borealis Polymers Oy, R & T, FIN-06101 Porvoo, Finland*

Received 14 September 1994; accepted 15 March 1995

Abstract

Part I of this series described the modeling and characterization of a reaction calorimeter designed for studying polymerizations under real process conditions. In this part, a calibration heater is used as a model reaction and it is shown how accurately the reaction rate can be determined with the calorimeter. Polymerization conditions strongly affect the sensitivity of the calorimetric measurements. After careful characterization of the calorimeter, polymerization reactions can be accurately followed, even when the reaction is started below the target temperature. The polymerization can be characterized during a small conversion interval at the outset of the polymerization. The special features of polymerizations are demonstrated and the typical process parameters such as viscosity, heat transfer properties and heat generation are presented for four types of polymerizations.

Keywords: Heat balance calorimeter; Polymerization; Polymerization calorimeter; Reaction calorimetry; Utilization of the calorimeter

List of symbols

A	heat transfer area/m^2
c_p	heat capacity of the cooling liquid/(kJ kg^{-1} K^{-1})
K_p	heat transfer coefficient/(W K^{-1})
$\dot{m}$	mass flow rate of the cooling liquid/(kg s^{-1})

---

[*] Corresponding author.

SSDI 0040-6031(95)02351-8

$\dot{Q}_c$	power input by the heater/W
$\dot{Q}_{conv}$	convective heat flow rate/W
$\dot{Q}_{pump}$	power input by the gear pump/W
T_j	jacket temperature/K
T_{j0}	jacket inlet temperature/K
T_p	pump heat temperature/K
T_r	reactor temperature/K
U	overall heat transfer coefficient/(W m^{-2} K^{-1})
$\Sigma(mc_p)_j$	heat capacity of the jacket/(J K^{-1})
$\Sigma(mc_p)_r$	heat capacity of the reactor/(J K^{-1})

1. Introduction

Part I of this series [1] described the modeling and characterization of a calorimeter especially designed for studying polymerizations under real process conditions. Viscosity increase of the reaction mass and fouling at the reactor wall are typical features of many polymerizations. The change in viscosity during the polymerization can be measured in a suitably equipped reaction calorimeter. The overall heat transfer coefficient also changes drastically when the viscosity changes. The change in the overall heat transfer coefficient, as well as the viscosity and the reaction rate, can be reliably measured on-line once the calorimeter has been properly characterized. An overview of reaction calorimetry can be found in the literature [2–5].

Reaction calorimetry has been used especially in the field of free radical polymerizations [6–9]. Heat balance calorimeters, which work on the principle of measuring the convective heat flow rate, have been used to monitor heat transfer properties during polymerization [10, 11]. One of the key aims of our study was to apply the knowledge of calorimeter design gathered from low temperature (50–70°C) applications to the construction of a heat balance calorimeter also suitable for high temperature applications (90–120°C). The broad temperature range available widens the scale of polyreactions that can be studied.

In the work reported here, the special features of polymerizations are demonstrated for four types of polymerizations. Typical process parameters such as viscosity, heat transfer properties and heat generation are presented.

2. Utilization of the calorimeter

Once a calorimeter has been properly characterized, it can be used to determine the essential parameters of polymerization reactions. The most important parameter is the reaction rate, which is calculated from the the heat generation of polymerization. In this study a calibration heater was used as a model reaction to show how accurately the reaction rate can be determined with the reaction calorimeter.

Typical temperature profiles are shown in Fig. 1. The temperature responds fairly slowly because the temperature controller is tuned to be very slow. The deviation of the base line is due to the convective heat flow rate and the heat accumulation terms. When the controller is tuned too fast the jacket inlet temperature swings widely because electromagnetic and magnetic fields of the pumps and thyristors cause disturbances in the recorded temperatures. This in turn causes wide variations in the characterization of the reaction. When the tuning is done carefully the deviation of the base line is due only to the heat accumulation terms. The tuning of the controller can be adjusted according to the reaction concerned.

Water was used as an inert fluid in the reaction calorimeter. The power input of the stirrer is neglected because the viscosity of the water is so low. Heat losses are also assumed to be negligible because there is no difference between the reactor and jacket temperatures. The simulation reaction is determined with Eq. (1)

$$\dot{Q}_c = \dot{Q}_{conv} - \dot{Q}_{pump} + K_p(T_j - T_p) + \dot{Q}_{accu,r} + \dot{Q}_{accu,j} \tag{1}$$

Convective heat flow rate is determined as

$$\dot{Q}_{conv} = \dot{m}(c_{pT_j}T_j - c_{pT_{j0}}T_{j0}) \tag{2}$$

and the power input by the gear pump is

$$\dot{Q}_{pump} = 107.1\,\mathrm{W}\text{-}(0.474\ \mathrm{W\ {}^{\circ}C^{-1}})\,T_j \tag{3}$$

The heat accumulation which is due to the ractor and the construction of the reactor is calculated as

$$\dot{Q}_{accu,r} = \Sigma(mc_p)_r\,\mathrm{d}T_r/\mathrm{d}t \tag{4}$$

and the heat accumulation which is due to the jacket and the construction of the inner jacket loop is calculated as

$$\dot{Q}_{accu,j} = \Sigma(mc_p)_j\,\mathrm{d}T_j/\mathrm{d}t \tag{5}$$

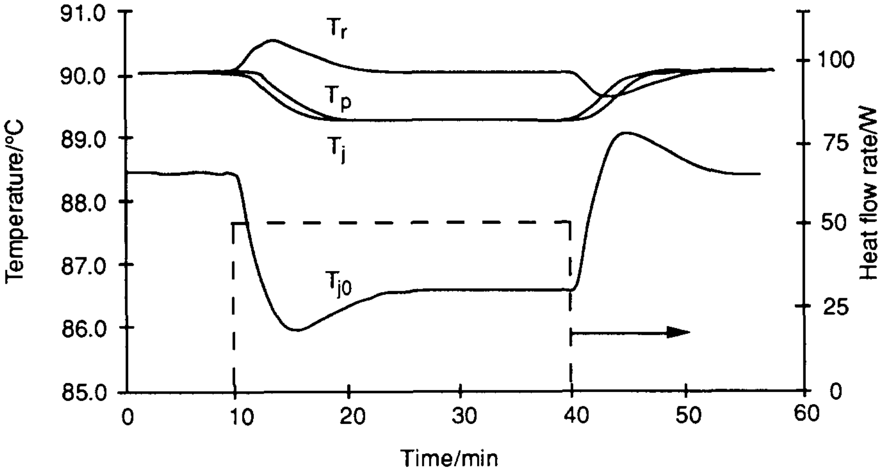

Fig. 1. Typical temperature profiles of the reaction. The calibration heater was switched on after 10 min and the duration of the simulation was 30 min. The power input of the calibration heater was set to 50 W.

For the same experimental conditions, Fig. 2 shows how the simulation reaction is determined by using the steady state assumption; heat accumulation terms are assumed to be negligible. It took almost 14 min, from 10 min to 24 min, before the steady state heat balance gave the right flow rate value. Fig. 2 shows that the steady state assumption is not enough for the study of polymerization reactions, particularly at the beginning.

Fig. 3 shows the improvement when heat accumulation terms (Eq. (1)) are included. There is only a slight time delay before the heat balance gives the right heat flow rate value. The reaction rate could be determined very accurately with the well-characterized reaction calorimeter, even during the small conversion interval at the very beginning of the polymerization.

The time delay in Fig. 3 is due to the slow rate of data acquisition (1/30 Hz). The rate needs to be slow because otherwise the heat accumulation terms make the base line worse. For example, the heat accumulation term of the jacket is calculated as $Q_{\mathrm{accu,j}} = \Sigma(mc_p)_{\mathrm{j}}\,\mathrm{d}T_{\mathrm{j}}/\mathrm{d}t$. The heat capacity of the jacket is 4490 J °C^{-1} and the resolution of the temperature measurement is 0.024°C (a theoretical value associated with the particular A/D converter and temperature measurement range). When the time interval of the derivative is 1 s, the deviation of the base line is ± 4490 J °C^{-1} × 0.024°C s^{-1} = ± 108 W. Fig. 4 shows how the base line depends on the data acquisition rate. The deviation of the base line is smaller than the theoretical value because the sensitivity of the temperature measurements is improved by the mathematical treatment. The base lines at four data acquisition rates are displayed in Fig. 4. As can be seen, the fastest data acquisition rate that could be used was 1/10 Hz;

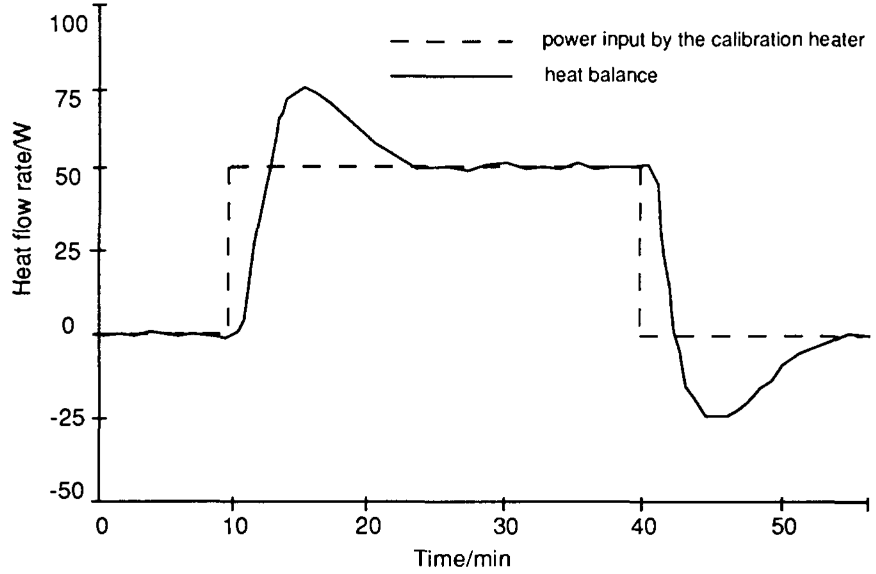

Fig. 2. Determination of the simulation reaction using the steady state assumption.

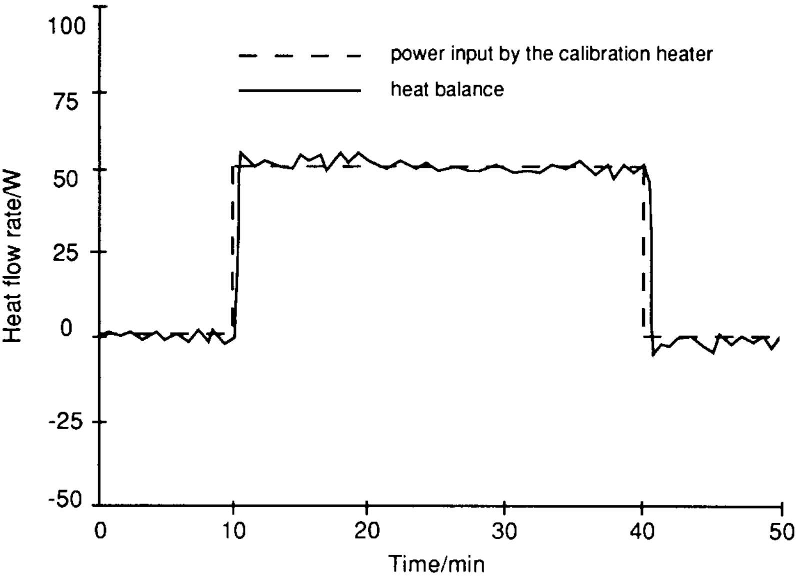

Fig. 3. Determination of the simulation reaction with Eq. (1).

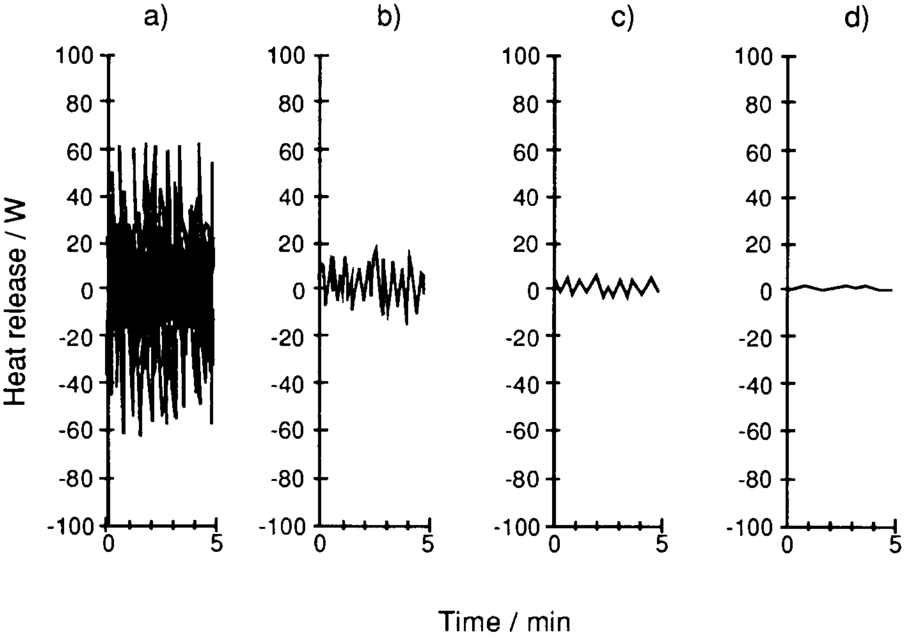

Fig. 4. Effect of the data acquisition rate on the deviation of the base line: (a) 1 Hz, (b) 1/5 Hz, (c) 1/10 Hz, (d) 1/30 Hz.

otherwise the determination became distorted by the deviation of the base line. With polymerization times generally in the order of several hours, this data acquisition rate is adequate.

Fig. 5 shows that if the gear pump is of heavy construction, it is essential to have the heat flow rate through the pump head included in the heat balance equation. For the experimental conditions shown, it took nearly 25 min before the calorimetric heat balance gave the right heat release when the heat flow rate through the pump head was not included. With this included, the right heat release was obtained almost immediately. Polymerization conditions strongly affect the calorimetric measurements. The heat accumulated in the reactor and the jacket is much less when the initiator is added at the polymerization temperature than when it is added before the polymerization temperature has been reached. When the calorimeter was properly characterized, the reaction rate could be measured accurately even during a small conversion interval at the beginning of the polymerization.

3. Application to polymerizations

The reaction calorimeter used for this study has been described in a previous paper [1]. The special features of polymerizations are now demonstrated for four types of reactions corresponding to the conditions shown in Table 1. The heat released during polymerization is determined according to Eq. (1). Changes in the reaction-side heat transfer coefficient can be allowed for in a heat balance (but not in a heat flow)

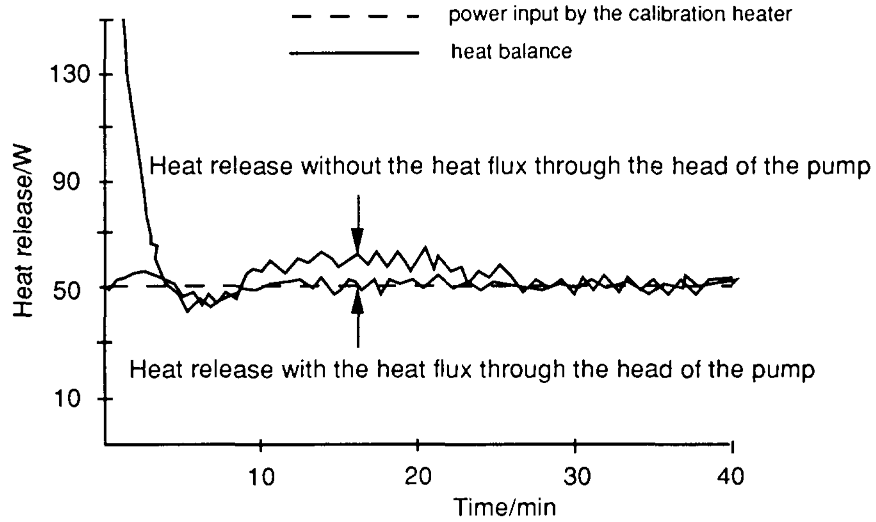

Fig. 5. Effect of the polymerization conditions on the calorimetric measurements. The power input of the calibration heater was set to 50 W. The water-filled reactor was heated up to the setpoint, which was 90°C. The heat balance calculation was started when the reactor temperature was 2 K below the setpoint.

Table 1
Conditions of polymerization

Properties	Exp. 1	Exp. 2	Exp. 3	Exp. 4
Polymerization type	Slurry	Suspension	Bulk	Solution
Monomer	Ethylene	Styrene	ε-Caprolactone	ε-Caprolactone
Temperature/K	333	363	383	373
Reaction medium	*n*-Heptane	Water	ε-Caprolactone	Toluene
Catalyst	Cp_2ZrCl_2	Benzoyl peroxide	Stannous octoate	Stannous octoate
Reaction time/h	1.5	4.5	5	6

calorimeter by following the apparent viscosity of the reaction medium and its change during the reaction through torque measurement at the stirrer shaft. The overall heat transfer coefficient was evaluated by combining the heat balance of the reactor and the heat balance of the jacket. The overall heat transfer coefficient can be determined according to Eq. (6)

$$U = \frac{\dot{Q}_{\mathrm{conv}} - \dot{Q}_{\mathrm{pump}} - K_{\mathrm{p}}(T_{\mathrm{j}} - T_{\mathrm{p}}) + \dot{Q}_{\mathrm{accu,j}}}{A(T_{\mathrm{r}} - T_{\mathrm{j}})} \tag{6}$$

3.1. Heat released by polymerization

Polymerizations are in general strongly exothermic. Fig. 6 compares the heat release during the polymerization of ethylene (exp. 1) measured as described in this paper and calculated from the known monomer mass flow rate, assuming a heat of reaction of 106 kJ mol^{-1}. The two are in excellent agreement and the heat of reaction is consistent with the literature values, 101–108 kJ mol^{-1} [12].

3.2. Viscosity

Compared with homogeneous bulk or solution polymerization, the increase in viscosity during polymerization in disperse systems is almost negligible in suspension polymerization and moderate in heterogeneous bulk polymerization.

Fig. 7 shows how the apparent viscosity changes during polymerization for the examples shown in Table 1.

In slurry polymerizations the viscosity increases sharply when the solid concentration is near to its maximum value. An example of this kind of situation is shown in Fig. 8. Ethylene polymerization was carried out with Cp_2ZrCl_2-methylaluminoxane catalyst. There was a rapid decrease in the free reaction medium during the polymerization, which caused the dramatic viscosity increase [13]. The viscosity increase was strongly dependent on the slurry concentration and on the shape of the polymer particles.

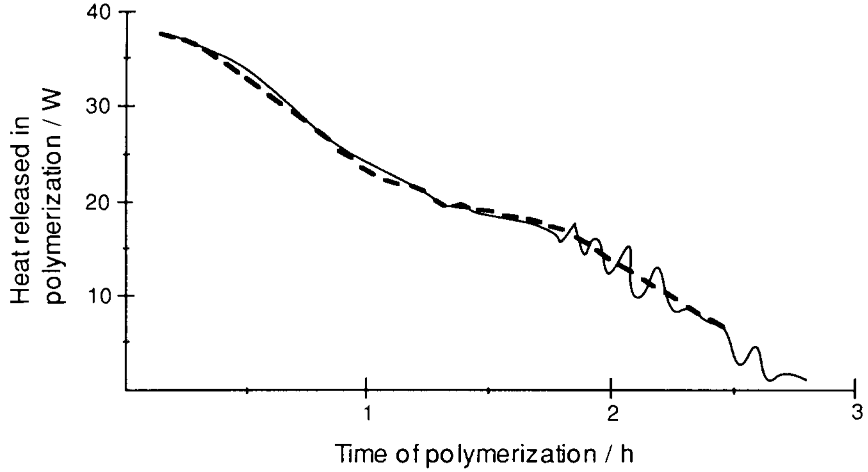

Fig. 6. Comparison of the heat released in the polymerization, measured by calorimeter (—) and calculated from ethylene mass flow rate (– – – –), $\Delta H = 106\ \text{kJ mol}^{-1}$. For description of run, see Table 1.

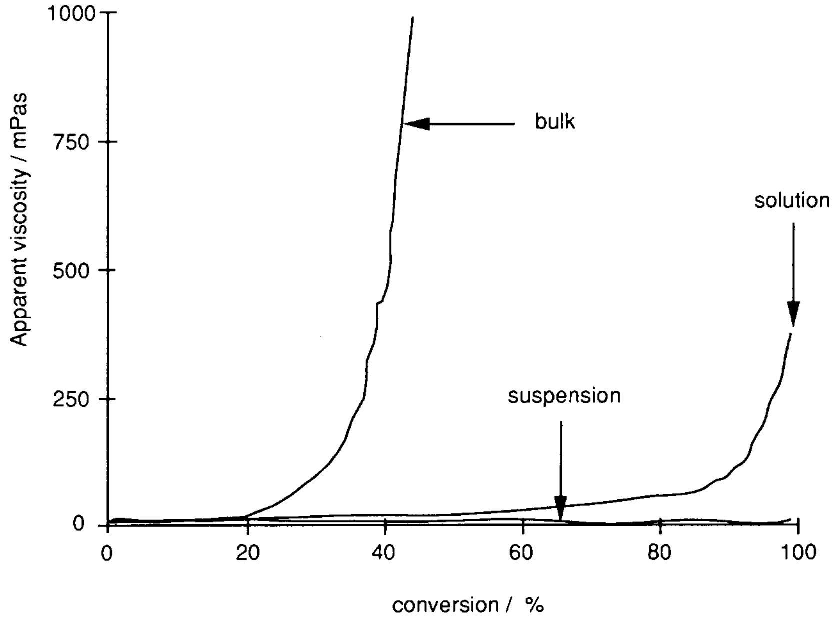

Fig. 7. Changes in viscosity during monomer conversion in bulk, suspension and solution processes. For description of runs, see Table 1.

3.3. *Heat transfer properties*

The accuracy of the calculated heat transfer coefficient was not so good at the beginning or at the end of the reaction as in the middle phase. At the beginning, measured temperatures oscillated slightly because of the lag of the temperature controller. At the end, the temperature differences were so small that the error in the temperature measurement became large. The viscosity may increase dramatically even at intermediate conversions and mixing becomes difficult, with the result that the heat transfer coefficients decrease with the progress of the polymerization. Fig. 9 shows the heat transfer coefficient plotted against monomer conversion for different polymerization processes. The conditions of the polymerizations are presented in Table 1.

In slurry polymerizations, changes in heat transfer properties are often neglected as there are only slight changes in viscosity during the course of the reaction. However, experiments investigating the heat transfer properties in ethylene slurry polymerization have shown that calorimetric measurements based on heat flow calorimetry (constant heat transfer coefficient) give distorted results if the heat transfer properties are assumed to be constant. Fig. 10 shows how large the deviation can be if the heat transfer coefficient is assumed to be constant.

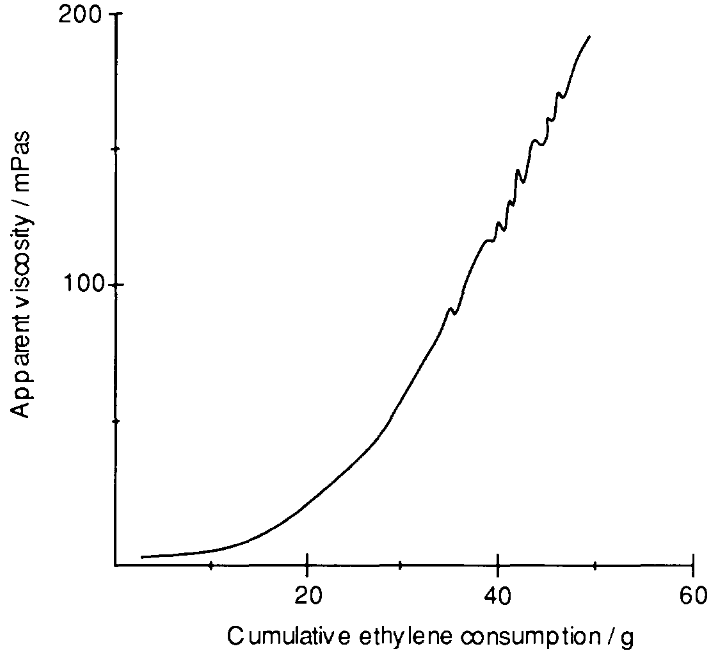

Fig. 8. Dependence of the apparent viscosity on the cumulative ethylene consumption in slurry polymerization. For description of run, see Table 1.

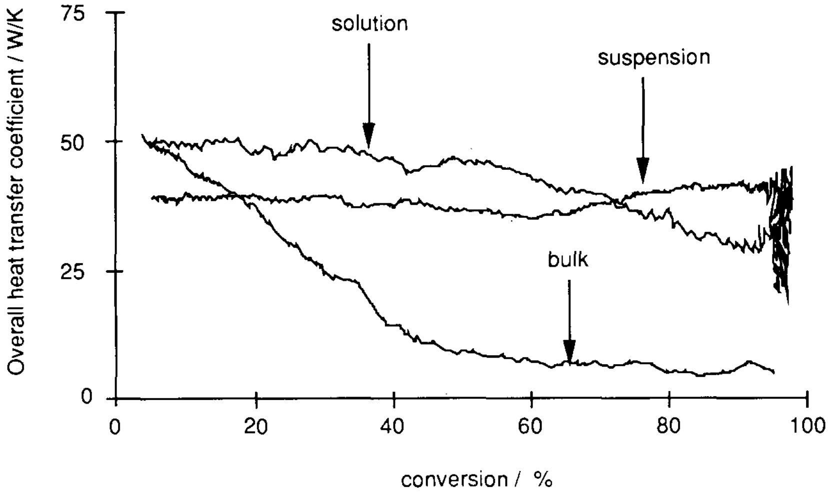

Fig. 9. Change in heat transfer coefficient with monomer conversion in different polymerization processes. For description of runs, see Table 1.

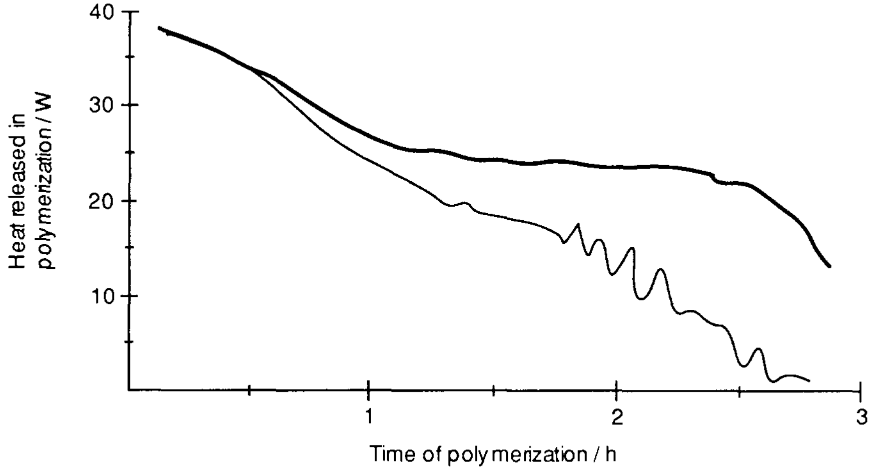

Fig. 10. Comparison of the heat released in the polymerization, measured by heat balance calorimeter (—) and heat flow calorimeter (—).

4. Conclusions

In heat balance calorimetry, the calorimetric measurements are the sum of the convective heat flow rate, the power input of the pump in the inner jacket loop, and the heat accumulation terms. Polymerization conditions strongly affect the sensitivity of the calorimetric measurements. The accuracy of the measurement is worse when the initiator is added to the polymerization system before heating it to the polymerization temperature than when it is added at the polymerization temperature. In the first case, when the system is heated to the polymerization temperature, it is especially important that the power input of the gear pump be estimated accurately. The power input of the gear pump can be 50–100 W, which is about three to five times as great as the calculated heat generation rate of the reaction. If the power input is incorrectly estimated, the on-line determinations of the device will not be accurate enough. The results could still be useful, however, if recalculated with the right power input of the pump. A careful characterization of the reaction calorimeter makes an accurate monitoring of the reaction possible even when the initiator is added before the polymerization temperature is reached.

The experimental results presented indicate that the most suitable reaction calorimeters for versatile polymerization process studies are heat balance calorimeters. These consist of a jacketed reactor allowing accurate measurement of jacket inlet and outlet coolant and reactor temperatures. Heat flow calorimeters, which measure the heat flow rate through the reactor wall, are not practical due to the strong variation of the reaction-side heat transfer coefficient in polymerization processes.

References

[1] M. Lahti, A. Avela and J. Seppälä, Polymerization calorimeter I. Modelling and characterization, Thermochim. Acta, in press.
[2] H.-U. Moritz, Habilitationsschrift, Technische Universität Berlin, 1988.
[3] H.-U. Moritz, in K.-H. Reichert and W. Geiseler (Eds.), Polymer Reaction Engineering, Proc. 3rd Berlin International Workshop on Polymer Reaction Engineering, VCH Publishers, New York, 1989, p. 248.
[4] L.G. Karlsen and J. Villadsen, Chem. Eng. Sci., 42 (1987) 1153.
[5] L.G. Karlsen and J. Villadsen, Chem. Eng. Sci., 42 (1987) 1165.
[6] C.-U. Schmidt and K.-H. Reichert, Chem. Ing. Technol., 59 (1987) 739.
[7] H.-G. Poersch-Panke, A. Avela and K.-H. Reichert, Chem. Ing. Technol., 61 (1989) 970.
[8] H.-G. Poersch-Panke, A. Avela and K.-H. Reichert, Angew. Makromol. Chem., 206 (1993) 157.
[9] H. Nilsson, C. Silvegren and B. Törnell, Angew. Makromol. Chem., 112 (1983) 125.
[10] H.-G. Poersch-Panke, A. Avela and K.-H. Reichert, Chem. Ing. Technol., 61 (1989) 808.
[11] T. Lewin and K.-H. Reichert, Chem. Ing. Technol., 65 (1993) 739.
[12] J. Brandrup and E.H. Immergut, Polymer Handbook, Interscience Publishers, New York, 1966.
[13] J. Koivumäki, M. Lahti and J. Seppälä, Angew. Makromol. Chem., 221 (1994) 117.